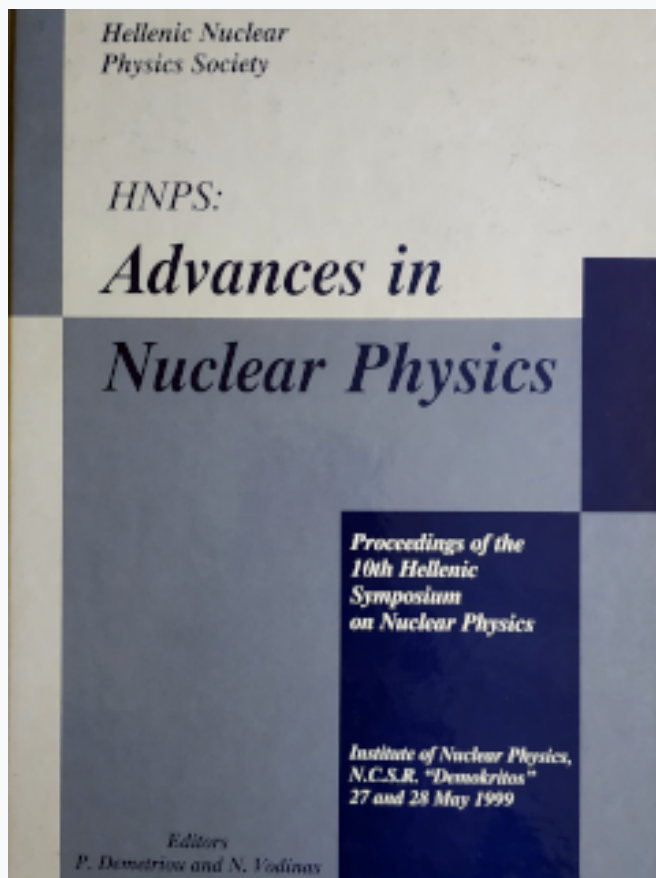


## HNPS Advances in Nuclear Physics

Vol 10 (1999)

HNPS1999



### Oxygen Contamination of Multilayer TiN<sub>x</sub> — SiO<sub>2</sub> — Si Structures found by Resonant RBS Analysis

X. A. Aslanoglou, E. Evangelou, N. Konofaos, Ch. Dimitriades, E. Kossionides, G. Kaliampakos, G. Kriembardis

doi: [10.12681/hnps.2241](https://doi.org/10.12681/hnps.2241)

#### To cite this article:

Aslanoglou, X. A., Evangelou, E., Konofaos, N., Dimitriades, C., Kossionides, E., Kaliampakos, G., & Kriembardis, G. (2020). Oxygen Contamination of Multilayer TiN<sub>x</sub> — SiO<sub>2</sub> — Si Structures found by Resonant RBS Analysis. *HNPS Advances in Nuclear Physics*, 10, 20–25. <https://doi.org/10.12681/hnps.2241>

# Towards ab initio structure and response calculations across the nuclear chart <sup>1</sup>

P. Papakonstantinou, R. Roth, H. Hergert, N. Paar

*Institute of Nuclear Physics, T.U. Darmstadt, Schlossgartenstr. 9,  
D-64289 Darmstadt, Germany*

---

## Abstract

Starting from the Argonne V18 nucleon-nucleon interaction and using the Unitary Correlation Operator Method, a correlated interaction  $v_{\text{UCOM}}$  has been constructed, which is suitable for calculations within restricted Hilbert spaces. In this work we employ the  $v_{\text{UCOM}}$  in Hartree-Fock, perturbation-theory and RPA calculations. First results are reported on the ground-state properties of various closed-shell nuclei, as well as some excited states. Our results provide valuable information on the properties of the  $v_{\text{UCOM}}$  and guidance to further optimization.

The above scheme offers the prospect of ab initio calculations in nuclei throughout the nuclear chart. It can be used in conjunction with other realistic NN interactions as well, both local and non-local. Various many-body methods can be employed, such as Second RPA, QRPA, Shell Model, etc.

---

## 1 Introduction

A major challenge in nuclear theory has been to describe nuclei and nuclear matter as interacting fermion systems, starting from the nucleon-nucleon interaction (NNI). This is particularly relevant now that realistic NNI parametrizations, which reproduce the experimental two-body data very accurately, have become available. The main problem in utilizing them in nuclear structure calculations is well known: the NNI induces strong short-range correlations (SRC) which cannot be described by simple (i.e., tractable also for heavy nuclei) wave functions. Fully microscopic calculations based on the realistic NNI are feasible numerically only for the lightest of nuclei (using the Green's Function Monte Carlo method or the no-core shell model) and for nuclear matter. Variational calculations are possible for the ground state of larger numbers of

---

<sup>1</sup> Work supported by the Deutsche Forschungsgemeinschaft, contract SFB 634

nucleons, with SRC included in the trial wave functions by means of correlation operators acting on simple many-body states. For heavier nuclei, one depends upon mean-field approaches and the shell model, where the starting point is a simple many-body wave function on top of which correlations and excitations are built; these approaches make use of effective NNIs. Extensive use is made of phenomenological effective interactions. The *ab initio* picture is lost and extrapolations to the unknown territories of the nuclear landscape become unreliable.

The Unitary Correlation Operator Method (UCOM) provides a novel scheme for carrying out nuclear structure and response calculations starting from realistic NNIs, across the nuclear chart (1; 2; 3; 4). As in other correlator-approaches, SRC are introduced in the nuclear wave function by means of a correlation operator  $C$ . This has the form  $C = C_\Omega C_r$ , where the operators  $C_r$  and  $C_\Omega$  describe the SRC induced by the strong repulsive core and the tensor part of the NN potential, respectively.  $C$  is state-independent and has an explicit operator form. The parameters entering the corresponding correlation functions are determined for each spin-isospin channel by minimizing the energy of the two-nucleon system. The correlation operator is unitary and can be used to introduce correlations into an uncorrelated  $A$ -body state or, alternatively, to perform a similarity transformation of an operator of interest. Applied to a realistic NN interaction, in particular, the method produces a “correlated” interaction,  $v_{\text{UCOM}}$ , which can be used as a universal effective interaction, for calculations within simple Hilbert spaces. The same transformation can then be applied to any other operator under study, as is needed for a consistent UCOM treatment. The  $v_{\text{UCOM}}$  is phase-shift equivalent to the bare interaction, by construction, and its matrix elements can be evaluated exactly (3; 4). Its low-momentum matrix elements are similar to those of  $V_{\text{low-}k}$ , the low-momentum interaction derived from bare realistic ones by employing renormalization group techniques (5).

The utilization of the UCOM involves a cluster expansion of the correlated operators and, currently, a truncation at the two-body level. The latter is justified by the short range of the correlations treated by the method. Indeed, the aim is to treat explicitly only the state-independent SRC; long-range correlations (LRC) should be described by the model space. The optimal separation of the two types of correlations remains an important task. It is expressed primarily by a constraint on the range of the tensor correlation functions, imposed during their parameterization. By varying this range (more precisely, the “correlation volume”  $I_\varphi^{(S,T)}$  (4)), a family of correlators and respective correlated interactions are obtained. Three-body interactions are currently not included. One way to account for three-body effects (genuine interactions, correlations, cluster terms) is by adding a simple phenomenological, non-local, two-body correction to the correlated Hamiltonian. The introduction of this correction, whose parameters are fixed by fitting ground-state properties of a small num-

ber of nuclei, has allowed the UCOM to successfully describe properties of nuclei up to mass numbers  $A \approx 60$ , in the framework of variational calculations within Fermionic Molecular Dynamics (3). Another possibility, currently under investigation, is to include a phenomenological, zero-range three-body interaction.

In this work we employ  $v_{\text{UCOM}}$  in Hartree-Fock (HF)- and RPA-based models, to study nuclear structure and response without restricting ourselves to light-to-medium systems. In Sec. 2 we present briefly the correlated interaction used. In Sec. 3 we report first results. We conclude in Sec. 4.

## 2 The correlated interaction

We consider correlated Hamiltonians based on the Argonne V18 (AV18) interaction (6) (without phenomenological corrections). In Fig. 1, the relative-momentum matrix elements of the bare and correlated ( $I_{\vartheta} = 0.09 \text{ fm}^3$ ) AV18 potential are depicted for the  $^1S_0$  and  $^3S_1 - ^3D_1$  channels. After the correlations are applied, off-diagonal matrix elements outside a band along the diagonal are strongly suppressed. For  $L = 0$  partial waves, the low-momentum matrix elements become strongly attractive.

In Ref. (4) we used correlated harmonic-oscillator (HO) matrix elements in exact no-core shell model (7) calculations for few-body systems. The matrix elements of the  $v_{\text{UCOM}}$  provide fast convergence. The bulk of the binding energy is already obtained in very small model spaces. By varying the range of the tensor correlations, we were able to map out the Tjon line and found that a  $v_{\text{UCOM}}$  of  $I_{\vartheta}^{(1,0)} = 0.09 \text{ fm}^3$  best reproduces the binding energy of the light nuclei  $^4\text{He}$ ,  $^3\text{H}$ ; the (1,1) channel is not relevant for these nuclei, therefore the range of the (generally much weaker) respective correlators could not be constrained at this stage.

## 3 Methods of calculation and results

The two-body matrix elements of the  $v_{\text{UCOM}}$  (without correction terms), Coulomb interaction and (intrinsic) kinetic energy are calculated in a HO basis. These are used as input in HF- and RPA-based calculations in configuration space. Only spherical, closed-shell nuclei have been considered so far. The following methods have been used:

**HF** - a spherical-HF method, to estimate at “zeroth order” the nuclear ground state (gs) properties. The HF single-particle wave functions are expanded

in the HO basis.

**HF+PT** - second order perturbation theory (PT) is performed on the HF basis to obtain a correction to the gs energy.

**HF+RPA** - a self-consistent model, which allows us to study collective excitations and to estimate a correction to the gs energy due to LRC.

**ERPA** - an extended RPA (8), which is built on top of the true RPA gs and involves an iterative solution of the RPA equations. Corrected single-particle energies and occupation numbers can be obtained, as well as excitation properties.

The PT and (E)RPA allow us to account for LRC, in addition to the SRC handled by the UCOM. The results presented in Figs. 2 and 3 were obtained using the optimal  $v_{\text{UCOM}}$  parameterization with  $I_{\vartheta}^{(1,0)} = 0.09 \text{ fm}^3$  and without (1,1) tensor correlators. The maximum HO-energy and angular-momentum quantum numbers used are  $N_{\text{max}} = 2n + \ell = 12$  and  $\ell_{\text{max}} = 10$ , respectively, providing a satisfactory degree of convergence.

### 3.1 Ground state properties

As shown in Fig. 2, binding is achieved already at the HF level. Inclusion of LRC corrections via PT brings the gs energy very close to the experimental data. RPA correlations result in overbinding (9), mainly due to the double-counting of second-order corrections inherent in the model. In general, tensor correlators of longer range (larger  $I_{\vartheta}$ ) provide stronger binding both at the HF and RPA level.

The HF single-particle levels (not shown) are too sparse. The omission of a three-body interaction and of LRC are responsible for this effect. Occupation numbers  $n_i = \langle a_i^\dagger a_i \rangle$  (in standard notation) have been calculated within ERPA for  $^{16}\text{O}$  and  $^{40}\text{Ca}$ . In principle, correlated operators  $C^\dagger a_i^\dagger a_i C$  should be used. The small depletion of the Fermi sea (of the order  $10^{-3}$ ) that we obtain using uncorrelated operators reflects the effect of the gs LRC (10).

### 3.2 Collective excitations

Our RPA results on the isoscalar giant monopole resonance (ISGMR), for various medium and heavy nuclei, are in good agreement with the experimental data. An example is shown in Fig. 3, where we see also that the gs correlations taken into account in ERPA have a small effect on the strength distribution. There are small differences between the calculated ISGMR centroid energies and the experimental ones (the calculated ones being 1-3 MeV too high). In general, lower  $I_{\vartheta}$  values result in lower ISGMR energies (9). The calculated

energy of the isovector giant dipole resonance within RPA (not shown) is too high compared with experiment; ERPA brings it somewhat lower, but not sufficiently to correct for this result. We found that the calculated energy of the IS giant quadrupole resonance is also too high. For these modes, involving oscillations of the nuclear density at the surface of the nucleus, an adequate treatment of LRC is important. Inclusion of  $2p2h$  configurations within Second RPA is expected to bring them to lower energies.

#### 4 Conclusions and perspectives

A correlated realistic interaction  $v_{\text{UCOM}}$ , constructed from the Argonne V18 potential using the Unitary Correlation Operator Method, is employed in HF- and RPA-based calculations. The performance of the  $v_{\text{UCOM}}$  is very encouraging. Certain aspects of the model (e.g., optimal tensor correlators, three-body effects) are still open to improvement. Other realistic NN interactions, local or non-local, can be used as well. More many-body methods will be employed in the future, such as Second RPA, in which the model space is extended, and thus accounts for LRC more effectively, and HF-Bogolyubov and QRPA, which will allow us to study nuclei between closed shells. The above scheme offers the prospect of ab initio calculations across the nuclear chart.

#### References

- [1] H. Feldmeier, T. Neff, R. Roth, J. Schnack, *Nucl. Phys. A* **632**, 61 (1998).
- [2] T. Neff, H. Feldmeier, *Nucl. Phys. A* **713**, 311 (2003).
- [3] R. Roth, T. Neff, H. Hergert, H. Feldmeier, *Nucl. Phys. A* **745**, 3 (2004).
- [4] R. Roth, H. Hergert, P. Papakonstantinou, T. Neff, H. Feldmeier, arXiv:nucl-th/0505080.
- [5] S.K. Bogner, T.T.S. Kuo, A. Schwenk, *Phys. Rep.* **386**, 1 (2003).
- [6] R.B. Wiringa, V.G. Stokes, R. Schiavilla, *Phys. Rev. C* **51**, 38 (1995).
- [7] P. Navrátil, G.P. Kamuntavicius, B.R. Barret, *Phys. Rev. C* **61**, 044001 (2000).
- [8] F. Catara, M. Grasso, G. Piccitto, M. Sambataro, *Phys. Rev. B* **58**, 16070 (1998).
- [9] N. Paar, P. Papakonstantinou, H. Hergert, R. Roth, Proc. LV National Conference on Nuclear Physics, "Frontiers in the Physics of Nucleus", St. Petersburg, Russia, 2005; arXiv:nucl-th/0506076.
- [10] A.N. Antonov, P.E. Hodgson and I.Zh. Petkov, *Nucleon Correlations in Nuclei*, Springer-Verlag, 1993.

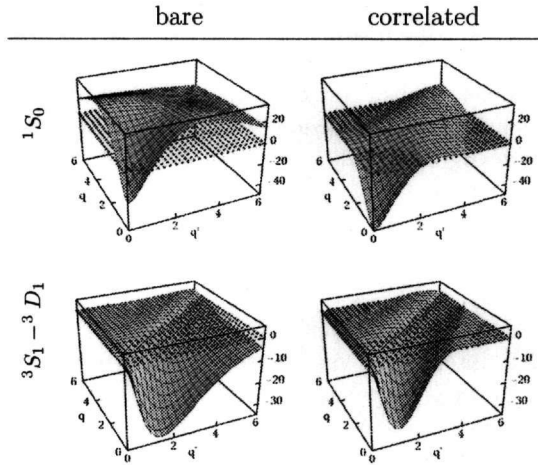


Fig. 1. Relative-momentum matrix elements  $\langle q(LS)JT | \dots | q'(L'S)JT \rangle$  of the bare AV18 potential (left-hand column) and the correlated one (right-hand column) in the partial waves  $^1S_0$  (upper row) and  $^3S_1-^3D_1$  (bottom row). The tensor correlator with  $I_\varphi = 0.09 \text{ fm}^3$  is used. Momenta  $q, q'$  are given in units of  $[\text{fm}^{-1}]$  and matrix elements in  $[\text{MeV}]$ . The dots mark the plane of vanishing matrix elements.

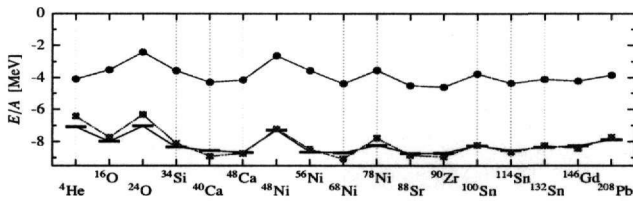


Fig. 2. Binding energy per nucleon, for the indicated nuclides, in HF (dots) and HF+PT (squares) and experimental (bars).

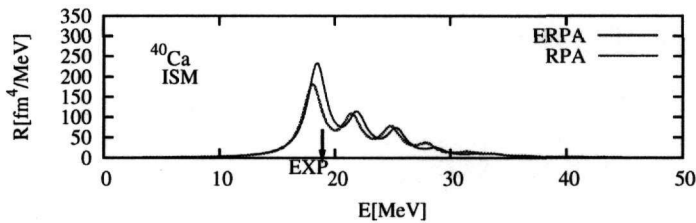


Fig. 3. Isoscalar monopole strength distribution of  $^{40}\text{Ca}$ , in HF+RPA (dashed lines) and ERPA (solid lines). An arrow indicates the experimental centroid of the ISGMR.